Table 1 Patient characteristics

	Overall (n=43)	Small LGE (n=21)	Large LGE (n=22)	p Value Small vs large
Age (years)	59±10	59±12	60±9	0.798
Male, n (%)	15 (35)	6 (29)	9 (41)	0.396
Body Mass Index (kg/m^2)	22.3±3.1	22.7±3.0	21.9±3.3	0.417
Systolic blood pressure (mm Hg)	123±18	126±17	120±18	0.250
Diastolic blood pressure (mm Hg)	72±12	71±11	73±13	0.642
NYHA functional class				0.875
I, n (%)	7 (16)	4 (19)	3 (14)	
II, n (%)	27 (63)	13 (62)	14 (64)	
III, n (%)	9 (21)	4 (19)	5 (23)	
IV, n (%)	0 (0)	0 (0)	0 (0)	
Organ involvement				
Lung, n (%)	9 (21)	4 (19)	5 (23)	0.767
Eye, n (%)	3 (7)	2 (10)	1 (5)	0.522
Skin, n (%)	2 (5)	1 (5)	1 (5)	0.973
Laboratory results at the beginning of steroid therapy				
White blood cell count (/μL)	5701±1587	5428±1288	5961±1820	0.276
Haemoglobin (g/dL)	13.4±1.5	13.3±1.6	13.4±1.3	0.709
Serum creatinine (mg/dL)	0.8±0.2	0.8±0.2	0.8±0.2	0.845
eGFR (mL/min/1.73m^2)	55±15	54±14	56±16	0.640
Albumin (g/dL)	4.1±0.3	4.0±0.3	4.1±0.3	0.573
Calcium (mg/dL)	9.5±0.4	9.4±0.2	9.6±0.6	0.311
BNP (pg/mL)	293±233	216±174	368±261	0.031
ACE (U/L)	14.7±8.4	15.0±9.2	14.4±7.6	0.843
Lysozyme (μg/mL)	8.0±4.1	7.2±3.2	8.9±5.0	0.222
Medications at the beginning of steroid therapy				
β blockers, n (%)	18 (42)	8 (38)	10 (45)	0.625
ACE inhibitors, n (%)	17 (40)	7 (33)	10 (45)	0.416
ARB, n (%)	9 (21)	4 (19)	5 (23)	0.767
Diuretics, n (%)	23 (53)	9 (43)	14 (64)	0.172
Antiarrhythmic agents, n (%)	9 (21)	5 (24)	4 (18)	0.650
Implanted devices at the beginning of steroid therapy				
Pacemaker, n (%)	7 (16)	5 (24)	2 (9)	0.191
Implantable cardioverter defibrillator, n (%)	7 (16)	3 (14)	4 (18)	0.729
Cardiac resynchronisation therapy, n (%)	2 (5)	0 (0)	2 (9)	0.157
Echocardiographic analysis				
LVEF (%)	41±10	45±11	36±6	0.001
LV diastolic dimension (mm)	57±8	52±6	61±8	<0.001
LV systolic dimension (mm)	44±9	39±8	49±7	<0.001
LV end-diastolic volume index (mL/m^2)	111±38	92±27	130±38	<0.001
LV end-systolic volume index (mL/m^2)	68±31	52±22	84±30	<0.001
CMR analysis				
LVEF (%)	38±12	43±12	32±10	0.002
LV end-diastolic volume index (mL/m^2)	112±42	92±27	132±45	0.001
LV end-systolic volume index (mL/m^2)	73±38	54±24	91±41	<0.001
LV mass (g)	130±38	122±47	138±27	0.195
LV mass index (g/m^2)	82±23	78±28	87±17	0.219
LGE mass (g)	26±16	14±11	38±11	<0.001
% LGE mass (%)	19±10	11±5	28±5	<0.001

ACE, angiotensin-converting enzyme; ARB, angiotensin II receptor blocker; BNP, B-type natriuretic peptide; CMR, cardiovascular magnetic resonance; eGFR, estimated glomerular filtration rate; LGE, late gadolinium enhancement; NYHA, New York Heart Association.

combined adverse outcomes (table 2). Additionally, multivariate analysis revealed that extent of LGE was an independent predictor of combined adverse outcomes (adjusted HR=1.10, 95% CI 1.01 to 1.21, p=0.021). In the present patient population, ROC curve analysis indicated that %LGE mass had the modest ability to predict combined adverse outcomes (AUC=0.77, 95% CI 0.60 to 0.89). A cutoff level of %LGE ≥21.9% best predicted combined adverse outcomes, with a sensitivity of 81.3% and a specificity of 70.3%. The test's positive and negative predictive values were 61.9% and 86.3%, respectively.

Association of extent of LGE with improvement in LV function after steroid therapy

Changes in LV end-diastolic volume index and LVEF from baseline to 6 months after steroid therapy are presented in figure 3. In the small-extent LGE group, LV end-diastolic volume index

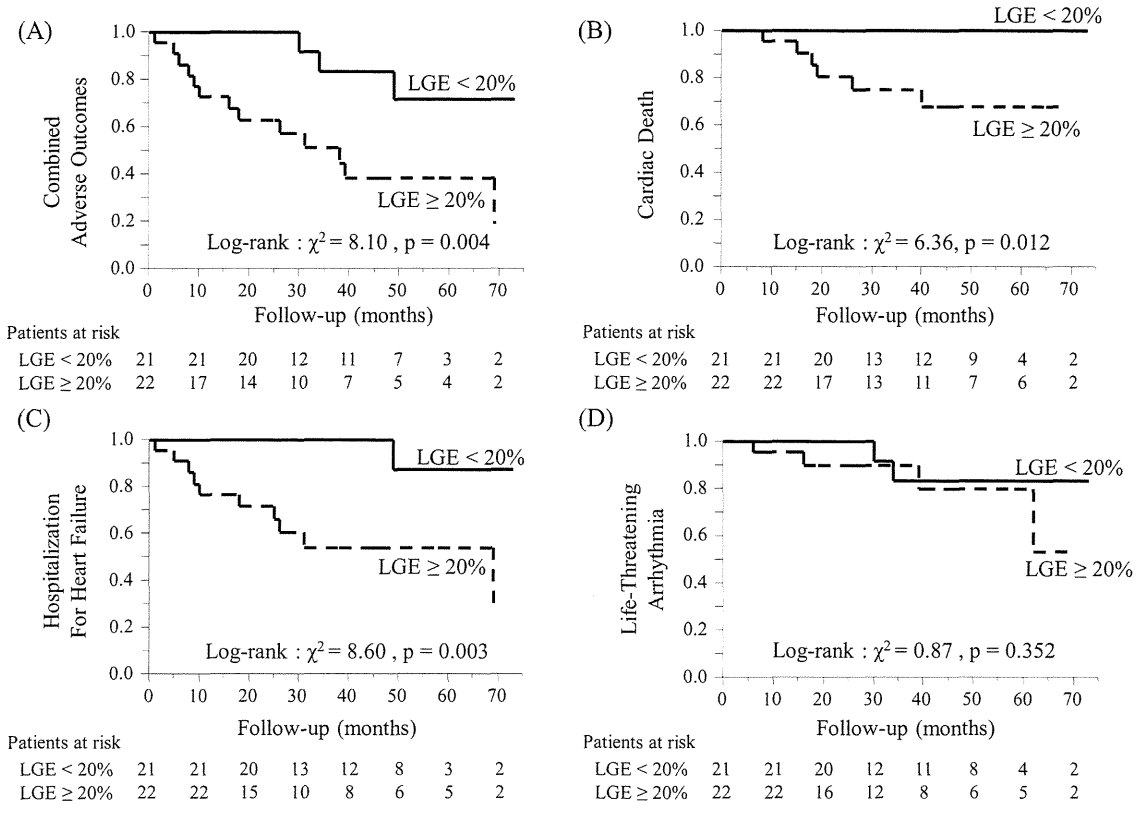

Figure 2 Kaplan–Meier cumulative event curves for (A) combined adverse outcomes, (B) cardiovascular deaths, (C) hospitalisation for heart failure, and (D) life-threatening arrhythmia. The combined adverse outcomes include cardiovascular deaths, hospitalisation for heart failure, and life-threatening arrhythmia. The log-rank p value for the difference between the Kaplan–Meier curves is shown.

significantly decreased (92±27 and 85±20 mL/m^2 before and after steroid therapy, respectively; p=0.005) and LVEF significantly increased (45±11 and 50±10% before and after steroid therapy, respectively; p<0.001) at 6 months after steroid therapy. However, in the large-extent LGE group, neither LV volumes nor LVEF changed substantially (LV end-diastolic volume index: 130±38 and 131±40 mL/m^2 before and after steroid therapy, respectively; p=0.731, LVEF: 36±6 and 35 ±8% before and after steroid therapy, respectively; p=0.213). Furthermore, regression analysis revealed a significant negative correlation between extent of LGE and changes in LVEF (r^2=0.38, p<0.001) (figure 4A). We observed an association between extent of LGE and changes in LVEF even after adjustment for LVEF before steroid therapy (r^2=0.43, p<0.001). On the other hand, a significant association was not found between changes in LVEF and pretherapy LVEF (p=0.145) (figure 4B).

DISCUSSION

LGE imaging by CMR has revolutionised the diagnosis of cardiomyopathies. Furthermore, in patients with sarcoidosis, this technique is also highly useful for the detection of myocardial involvement. Since the extent of LGE can now be quantified by commercially available software, we attempted to clarify the prognostic impact of quantitative evaluation of LGE in CS patients in the present study. We obtained evidence that the extent of LGE before steroid therapy was inversely correlated with improvement in LVEF at 6 months after steroid therapy, and that a larger extent of LGE predicted a higher incidence of cardiac events, even after adjustment for LVEF.

Prediction of adverse outcomes

It has been reported that survival of CS patients with preserved LVEF is better than that of patients with low LVEF.[14 20] Recently, the prognostic capability of LGE imaging for predicting outcomes has been assessed. It has been shown that the presence of LGE predicts adverse outcomes in patients with dilated cardiomyopathy[21 22] and in patients with hypertrophic cardiomyopathy.[23–25]

In patients with systemic sarcoidosis, Greulich *et al* and Patel *et al* reported that the presence of myocardial LGE can predict adverse cardiac outcomes.[7 10] However, in their study patients, systemic sarcoidosis was diagnosed on the basis of involvement of organs other than the heart; therefore, many patients without myocardial involvement were included. In patients with CS, granulomatous inflammation and myocardial fibrosis tend to develop during the early stages of the disease. Since LGE reflects myocardial fibrosis and granulomatous inflammation,[7] most CS patients may have a certain extent of LGE when they were diagnosed with CS.[6] Indeed, our study demonstrated that, among the 50 patients who were diagnosed with CS according to the guideline[11] and underwent CMR in our hospital, 96 percent of the patients did have LGE, and that their baseline characteristics revealed relatively advanced myocardial impairment compared with those reported in previous studies.[7 10] We therefore hypothesised that quantitative evaluation of LGE would be useful for the prediction of cardiac events in CS patients. The results of the present study demonstrated that CS patients with a large extent of LGE had a high incidence of adverse outcomes, including cardiac death and hospitalisation for heart failure.

Table 2 Univariate and multivariate Cox proportional hazards models for combined adverse outcomes including cardiac death, hospitalisation for heart failure, and life-threatening arrhythmias

	Univariate analysis		Multivariate analysis	
Variable	**Unadjusted HR (95% CI)**	**p Value**	**Adjusted HR(95%CI)**	**p Value**
Age*	1.07 (0.71 to 1.74)	0.765	–	–
Male	1.75 (0.63 to 4.87)	0.279	–	–
NYHA functional class†	2.45 (1.08 to 5.73)	0.032	2.40 (1.04 to 5.80)	0.040
eGFR‡	1.00 (0.96 to 1.03)	0.852	–	–
BNP§	5.60 (1.19 to 30.9)	0.028	0.71 (0.10 to 5.43)	0.740
CMR analysis				
LVEF¶	0.80 (0.62 to 1.00)	0.049	0.89 (0.67 to 1.19)	0.463
LV end-diastolic volume index**	1.08 (0.96 to 1.21)	0.203	–	–
LV end-systolic volume index**	1.13 (0.99 to 1.26)	0.065	–	–
LV mass index††	1.00 (0.81 to 1.21)	0.979	–	–
% LGE mass¶	1.71 (1.26 to 2.47)	0.001	1.64 (1.10 to 2.66)	0.015

Multivariable model included NYHA functional class, BNP, LVEF and %LGE mass.
*HR reflects risk with an increase of 10 years.
†With an increase of 1 functional class.
‡With an increase of 1 mL/min/1.73 m^2.
§With an increase of 1 logBNP.
¶With an increase of 5%.
**With an increase of 10 mL/m^2.
††With an increase of 10 g/m^2.
BNP, B-type natriuretic peptide; CMR, cardiovascular magnetic resonance; eGFR, estimated glomerular filtration rate; LGE, late gadolinium enhancement. NYHA, New York Heart Association.

In this study, approximately 25% of the CS patients required hospitalisation for heart failure during the follow-up period. Furthermore, 45% of these patients died of refractory heart failure. The extent of LGE indicates the severity of myocardial fibrosis, which is linked to the severity of LV dysfunction.[26 27] Therefore, the presence of large-extent LGE could predict refractory heart failure in CS patients. On the other hand, life-threatening arrhythmias occurred in 14% of these patients with CS. The frequency of life-threatening arrhythmias was higher in the large-extent LGE group, although the difference was not significant. Even localised lesions in the myocardium could be origins of re-entry arrhythmias, regardless of the extent of LGE, that is, myocardial fibrosis. In fact, in this study population, two patients with small-extent LGE who had a localised lesion in the LV septum or apex showed symptomatic ventricular tachyarrhythmias. This may imply that even small amounts of LGE can precipitate arrhythmias, whereas heart failure tends to occur when LGE is more extensive.

Prediction of improvement in LV function

Although little is known about the overall beneficial or adverse effects of steroid therapy in patients with CS, it has been reported that such patients with mildly to moderately reduced LVEF (30–54%) showed improvement in LV function after steroid therapy to a greater extent than that in patients with CS with severely reduced LVEF,[19] suggesting that adequate improvement in myocardial function cannot be expected in patients with severe myocardial impairment. In patients with dilated or ischaemic cardiomyopathy, a smaller extent of LGE, indicating a low degree of myocardial impairment, has been reported to be an indicator of recovery of LV systolic function.[28 29] In the present study, extent of LGE predicted improvement in LVEF in patients with CS after steroid therapy, being consistent with previous reports.

Autopsy findings in patients with CS in a previous study showed that LGE represents fibrosis and granulomatous inflammation in the myocardium.[7] Considering our results showing

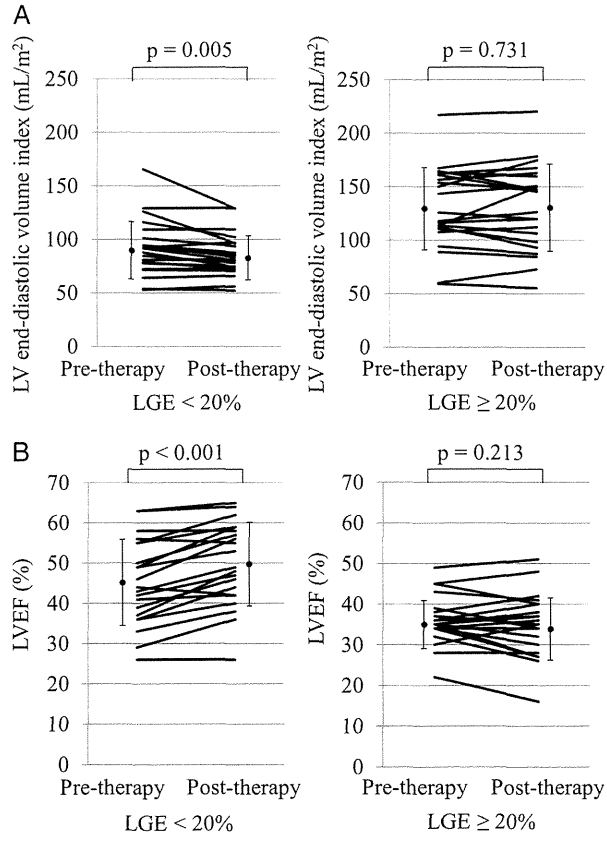

Figure 3 Alterations in LV end-diastolic dimensions (A) and LVEF (B) after steroid therapy.

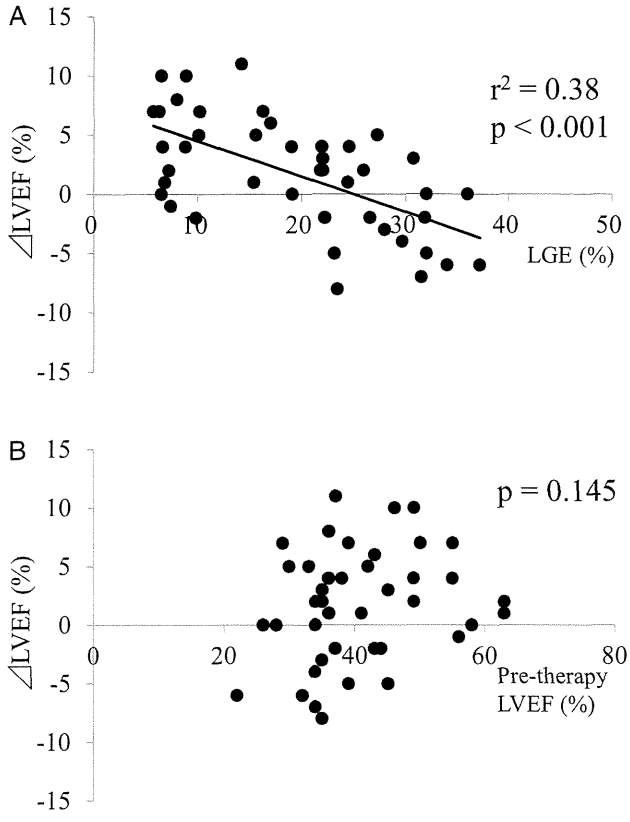

Figure 4 Relationship between the extent of late gadolinium enhancement (LGE) and changes in LVEF.

that patients with large-extent LGE before steroid therapy had no improvement in LVEF, LGE appears to reflect the degree of irreversible myocardial damage rather than granulomatous inflammation. In fact, in this study, some patients with severely reduced LVEF and mild LGE showed a good response to steroid therapy, suggesting that extent of LGE is a useful indicator of the expected improvement in LVEF, independent of LVEF before steroid therapy.

Study limitations

Several limitations to this study should be acknowledged. This was a single-centre retrospective observational study, and only patients who underwent CMR imaging before steroid therapy were enrolled. The results of the present study are limited by the small sample size and number of events. Some patients with CS who required a mechanical device, such as a pacemaker or implantable cardioverter-defibrillator for urgent conduction blocks or ventricular tachyarrhythmia at the initial visit, could not undergo CMR. There is a possibility that patients prone to arrhythmia events have therefore been excluded.

CONCLUSIONS

We conclude that the presence of large-extent LGE in patients with CS is linked to the absence of LV functional improvement and a high incidence of adverse outcomes after steroid therapy. We suggest that CMR imaging is useful for establishing the diagnosis of CS and also for predicting adverse events and the efficacy of steroid therapy.

Key messages

What is known on this subject?
Late gadolinium enhancement (LGE) on cardiac MRI is an emerging tool for the diagnosis of cardiac sarcoidosis (CS).

What might this study add?
We suggest that cardiac MRI is useful for establishing the diagnosis of CS and also for predicting adverse events and the efficacy of steroid therapy.

How might this impact on clinical practice?
The prognostic impact of LGE in patients with CS after steroid therapy has not been well investigated. We demonstrated that large-extent LGE in patients with CS is linked to the absence of LV functional improvement and a high incidence of adverse outcomes after steroid therapy.

Contributors The contribution of each author is as follows; conception and design or analysis or analysis and interpretation of data, TI, TH YM and NY. Drafting of the manuscript or revising it critically for important content, TI, TH, NY, AF, HT, MA, HK, HO, SK and WS. Final approval of the manuscript submitted, TA and MK.

Funding This work was supported by grants-in-aid from the Ministry of Health, Labor, and Welfare-Japan (H23-Nanchi-Ippan-22 to MK), grants-in-aid from the Ministry of Education, Culture, Sports, Science and Technology-Japan (21390251 to MK), grants from the Japan Heart Foundation (MK), and grants from the Japan Cardiovascular Research Foundation (MK).

Competing interests None.

Patient consent Obtained.

Ethics approval The ethics committee of National Cerebral and Cardiovascular Center.

Provenance and peer review Not commissioned; externally peer reviewed.

REFERENCES

1 James DG, Neville E, Carstairs LS. Bone and joint sarcoidosis. *Semin Arthritis Rheum* 1976;6:53–81.
2 Johns CJ, Michele TM. The clinical management of sarcoidosis. A 50-year experience at the Johns Hopkins Hospital. *Medicine* 1999;78:65–111.
3 Shammas RL, Movahed A. Sarcoidosis of the heart. *Clin Cardiol* 1993;16:462–72.
4 Sharma OP, Maheshwari A, Thaker K. Myocardial sarcoidosis. *Chest* 1993;103:253–8.
5 Perry A, Vuitch F. Causes of death in patients with sarcoidosis. A morphologic study of 38 autopsies with clinicopathologic correlations. *Arch Pathol Lab Med* 1995;119:167–72.
6 Smedema JP, Snoep G, van Kroonenburgh MP, *et al*. Evaluation of the accuracy of gadolinium-enhanced cardiovascular magnetic resonance in the diagnosis of cardiac sarcoidosis. *J Am Coll Cardiol* 2005;45:1683–90.
7 Patel MR, Cawley PJ, Heitner JF, *et al*. Detection of myocardial damage in patients with sarcoidosis. *Circulation* 2009;120:1969–77.
8 Smedema JP, Snoep G, van Kroonenburgh MP, *et al*. The additional value of gadolinium-enhanced MRI to standard assessment for cardiac involvement in patients with pulmonary sarcoidosis. *Chest* 2005;128:1629–37.
9 Mahrholdt H, Wagner A, Judd RM, *et al*. Delayed enhancement cardiovascular magnetic resonance assessment of non-ischaemic cardiomyopathies. *Eur Heart J* 2005;26:1461–74.
10 Greulich S, Deluigi CC, Gloekler S, *et al*. CMR imaging predicts death and other adverse events in suspected cardiac sarcoidosis. *JACC Cardiovasc Imaging* 2013;6:501–11.
11 Hiraga H, Yuwai K, Hiroe M. *Guideline for the diagnosis of cardiac sarcoidosis: study report on diffuse pulmonary diseases (in Japanese)*. Tokyo, Japan: The Japanese Ministry of Health and Welfare, 1993:23–4.
12 Levey AS, Bosch JP, Lewis JB, *et al*. A more accurate method to estimate glomerular filtration rate from serum creatinine: a new prediction equation. Modification of diet in renal disease study group. *Ann Intern Med* 1999;130:461–70.
13 Matsuo S, Imai E, Horio M, *et al*. Revised equations for estimated gfr from serum creatinine in Japan. *Am J Kidney Dis* 2009;53:982–92.

14 Yazaki Y, Isobe M, Hiroe M, *et al*. Prognostic determinants of long-term survival in Japanese patients with cardiac sarcoidosis treated with prednisone. *Am J Cardiol* 2001;88:1006–10.
15 Lang RM, Bierig M, Devereux RB, *et al*. Recommendations for chamber quantification: a report from the American Society of Echocardiography's Guidelines and Standards Committee and the Chamber Quantification Writing Group, developed in conjunction with the European Association of Echocardiography, a branch of the European Society of Cardiology. *J Am Soc Echocardiogr* 2005;18:1440–63.
16 Amano Y, Kumita S, Takayama M, *et al*. Comparison of contrast-enhanced MRI with iodine-123 BMIPP for detection of myocardial damage in hypertrophic cardiomyopathy. *AJR Am J Roentgenol* 2005;185:312–18.
17 Kono AK, Yamada N, Higashi M, *et al*. Dynamic late gadolinium enhancement simply quantified using myocardium to lumen signal ratio: normal range of ratio and diffuse abnormal enhancement of cardiac amyloidosis. *J Magn Reson Imaging* 2011;34:50–5.
18 Bondarenko O, Beek AM, Hofman MB, *et al*. Standardizing the definition of hyperenhancement in the quantitative assessment of infarct size and myocardial viability using delayed contrast-enhanced CMR. *J Cardiovasc Magn Reson* 2005;7:481–5.
19 Gao P, Yee R, Gula L, *et al*. Prediction of arrhythmic events in ischemic and dilated cardiomyopathy patients referred for implantable cardiac defibrillator: evaluation of multiple scar quantification measures for late gadolinium enhancement magnetic resonance imaging. *Circ Cardiovasc Imaging* 2012;5:448–56.
20 Chiu CZ, Nakatani S, Zhang G, *et al*. Prevention of left ventricular remodeling by long-term corticosteroid therapy in patients with cardiac sarcoidosis. *Am J Cardiol* 2005;95:143–6.
21 Gulati A, Jabbour A, Ismail TF, *et al*. Association of fibrosis with mortality and sudden cardiac death in patients with nonischemic dilated cardiomyopathy. *JAMA* 2013;309:896–908.
22 Assomull RG, Prasad SK, Lyne J, *et al*. Cardiovascular magnetic resonance, fibrosis, and prognosis in dilated cardiomyopathy. *J Am Coll Cardiol* 2006;48:1977–85.
23 O'Hanlon R, Grasso A, Roughton M, *et al*. Prognostic significance of myocardial fibrosis in hypertrophic cardiomyopathy. *J Am Coll Cardiol* 2010;56:867–74.
24 Bruder O, Wagner A, Jensen CJ, *et al*. Myocardial scar visualized by cardiovascular magnetic resonance imaging predicts major adverse events in patients with hypertrophic cardiomyopathy. *J Am Coll Cardiol* 2010;56:875–87.
25 Rubinshtein R, Glockner JF, Ommen SR, *et al*. Characteristics and clinical significance of late gadolinium enhancement by contrast-enhanced magnetic resonance imaging in patients with hypertrophic cardiomyopathy. *Circ Heart Fail* 2010;3:51–8.
26 Butler CR, Kumar A, Toma M, *et al*. Late gadolinium enhancement in cardiac transplant patients is associated with adverse ventricular functional parameters and clinical outcomes. *Can J Cardiol* 2013;29:1076–83.
27 Motoyasu M, Kurita T, Onishi K, *et al*. Correlation between late gadolinium enhancement and diastolic function in hypertrophic cardiomyopathy assessed by magnetic resonance imaging. *Circ J* 2008;72:378–83.
28 Leong DP, Chakrabarty A, Shipp N, *et al*. Effects of myocardial fibrosis and ventricular dyssynchrony on response to therapy in new-presentation idiopathic dilated cardiomyopathy: insights from cardiovascular magnetic resonance and echocardiography. *Eur Heart J* 2012;33:640–8.
29 Kim RJ, Wu E, Rafael A, *et al*. The use of contrast-enhanced magnetic resonance imaging to identify reversible myocardial dysfunction. *N Engl J Med* 2000;343:1445–53.

ORIGINAL RESEARCH

American Heart Association | American Stroke Association.

Decreased Myocardial Dendritic Cells is Associated With Impaired Reparative Fibrosis and Development of Cardiac Rupture After Myocardial Infarction in Humans

Toshiyuki Nagai, MD, PhD;* Satoshi Honda, MD;* Yasuo Sugano, MD, PhD; Taka-aki Matsuyama, MD, PhD; Keiko Ohta-Ogo, MD, PhD; Yasuhide Asaumi, MD, PhD; Yoshihiko Ikeda, MD, PhD; Kengo Kusano, MD, PhD; Masaharu Ishihara, MD, PhD, FACC; Satoshi Yasuda, MD, PhD; Hisao Ogawa, MD, PhD, FACC; Hatsue Ishibashi-Ueda, MD, PhD; Toshihisa Anzai, MD, PhD, FACC, FAHA

***Background*—**Dendritic cells (DC) play pivotal roles in regulating the immune system and inflammatory response. We previously reported DC infiltration in the infarcted heart and its immunoprotective roles in the post-infarction healing process after experimental myocardial infarction (MI). However, its clinical significance has not been determined.

***Methods and Results*—**The degree of DC infiltration and its correlation with the post-infarction healing process in the human infarcted heart were investigated in 24 autopsy subjects after ST-elevation MI. Patients were divided into two groups according to the presence (n=13) or absence (n=11) of cardiac rupture. The numbers of infiltrated DC and macrophages and the extent of fibrosis in the infarcted area were examined. In the rupture group, $CD68^+$ macrophage infiltration was increased and $CD209^+$ DC, and $CD11c^+$ DC infiltration and the extent of reparative fibrosis were decreased compared with the non-rupture group, under matched baseline characteristics including the time from onset to death and use of revascularization. Furthermore, there was a significant positive correlation between the number of infiltrating $CD209^+$ DC, and $CD11c^+$ DC and the extent of reparative fibrosis.

***Conclusions*—**Decreased number of DC in human-infarcted myocardial tissue was associated with increased macrophage infiltration, impaired reparative fibrosis, and the development of cardiac rupture after MI. These findings suggest a protective role of DC in post-MI inflammation and the subsequent healing process. **(*J Am Heart Assoc.* 2014;3:e000839 doi: 10.1161/JAHA.114.000839)**

Key Words: cardiac rupture • dendritic cell • inflammation • myocardial infarction • reparative fibrosis

Early reperfusion of the infarcted tissue and reparative fibrosis are essential in preserving the structural integrity of the left ventricle (LV) after myocardial infarction (MI). Cardiac accommodation following MI occurs in different phases, which include inflammatory, early healing, and myocardial remodeling phases.[1,2] An inadequate healing process after MI would result in complications such as cardiac rupture, LV aneurysm, and congestive heart failure due to exaggerated LV remodeling. However, the precise mechanisms and the potential therapeutic targets in the post-MI healing process remain to be clarified.

We previously reported that higher concentrations of serum C-reactive protein (CRP)[3] and plasma interleukin (IL)-6[4] and peripheral monocytosis[5] predict a worse clinical outcome after MI, suggesting that an immune-mediated inflammatory response may adversely affect post-infarction healing and LV remodeling. Recently, we elucidated that dendritic cells (DC) infiltrated into myocardial tissue play immunoprotective roles in post-infarction healing and LV remodeling in animal models.[6,7]

DC are professional antigen-presenting cells (APC), which are found in all organ systems, including the myocardium. Several subtypes have been described thus far, with so-called myeloid DC (mDC) and plasmacytoid DC (pDC) being predominant.[8] We have demonstrated infiltration of mature activated mDC in the infarcted rat heart, peaking on day 7.[6] To elucidate the significance of DC, we generated a mouse model with selective depletion of bone marrow-derived DC,

From the Departments of Cardiovascular Medicine (T.N., S.H., Y.S., Y.A., K.K., M.I., S.Y., H.O., T.A.) and Clinical Pathology (T.M., K.O.-O., Y.I., H.I.-U.), National Cerebral and Cardiovascular Center, Osaka, Japan; Department of Cardiovascular Medicine, Graduate School of Medical Sciences, Kumamoto University, Kumamoto, Japan (H.O.).

*Dr Nagai and Dr Honda were equally contributed to the present study.

Correspondence to: Toshihisa Anzai, MD, PhD, FACC, FAHA, Department of Cardiovascular Medicine, National Cerebral and Cardiovascular Center, 5-7-1 Fujishiro-dai, Suita, Osaka 565-8565, Japan. E-mail: anzai@ncvc.go.jp

Received January 29, 2014; accepted April 28, 2014.

and demonstrated that the depletion of bone marrow-derived DC exacerbated post-infarction LV remodeling in association with enhanced inflammatory cytokine expression and matrix metalloproteinase (MMP)-9 activation via marked infiltration of proinflammatory monocytes ($Ly6C^{high}$) and classically activated M1 macrophages into the infarcted myocardium. On the contrary, decreased IL-10, which has anti-inflammatory activity and myocardial infiltration of anti-inflammatory monocytes ($Ly6C^{low}$) and alternatively activated M2 macrophages were observed in a rodent model.[7] These findings suggest that DC may play a protective role against post-infarction LV remodeling by regulating the homeostasis of monocytes and macrophages during the transition from inflammation to repair. However, the presence and the clinical significance of DC in the human infarcted heart remain to be determined.

In the present study, we used immunostaining techniques to identify and quantify DC infiltration in the infarcted myocardium in human autopsy samples, to clarify the impact of DC infiltration on the post-MI healing process and the development of cardiac rupture.

Methods

Patients

Among patients who were admitted to our institution with ST-elevation MI (STEMI) and underwent autopsy between December 1978 and May 1998 (n=49), 24 cases with enough preserved infarcted tissue for immunohistochemical analyses were examined.

All autopsies were performed within 24 hours after death. Heart tissue samples were taken from the LV infarcted area of patients who died of cardiac rupture including free wall rupture (n=9) and ventricular septal perforation (n=4), pump failure (n=10), or fatal ventricular arrhythmias (n=1). Patients were divided into two groups according to the presence (n=13) or absence (n=11) of cardiac rupture.

Our study was approved by the ethics committee of the National Cerebral and Cardiovascular Center, and conformed to the principles of the Declaration of Helsinki.

Histological and Immunohistochemical Staining

The ventricular tissue was fixed in formalin and embedded in paraffin using standard histological procedures. The tissue was cut to yield 5-μm-thick cross sections. The sections were subsequently stained with hematoxylin and eosin (HE) and Masson's trichrome staining to determine the extent of fibrosis.

Immunohistochemical examinations were performed on 5-μm-thick formalin-fixed and paraffin-embedded tissue sections. All steps were performed on a Leica Bond III automated system (Leica Microsystems) according to the manufacturer's instructions. In brief, specimens were deparaffinized and antigen was retrieved on the instrument. All slides were incubated with primary antibodies against CD68 (diluted 1:1000; Dako), CD209 (1:1000; BD Pharmingen), or CD11c (1:100; GeneTex) for 16 min, followed by incubation with a mouse-rabbit-horseradish peroxidase polymer and 3,3′-diaminobenzidine substrate. The sections were then incubated in primer (anti-rabbit and anti-mouse) for 8 minutes. Antibody binding was visualized using the avidin-biotin complex method according to the manufacturer's instructions (Vectastain ABC; Vector). The primary antibody was omitted from these protocols as a negative control. The sections were subsequently counterstained with HE.

Quantitative Analyses of Myocardial Inflammatory Cell Infiltration and Tissue Fibrosis

Stained inflammatory cells were counted in the infarcted area of each sample at a magnification of ×100 and in each of ten representative sections (0.1 mm^2), which were randomly chosen from infarct tissue without hemorrhagic change, using ImageJ software (version 1.38x; National Institutes of Health). For each sample, median cell numbers were calculated. For LV tissue fibrosis, percent area fraction (%AF) was measured using ImageJ software. These quantitative analyses were performed by two trained technicians without knowledge of patients' backgrounds.

Statistical Analysis

Continuous data were expressed as mean values±SD. The two groups were compared using the Wilcoxon rank sum test for continuous variables. Categorical variables were reported as frequencies with percentages and compared between the two groups using the Fisher's exact test. The correlation among the infiltration of $CD68^+$ macrophages, $CD209^+$ DC, $CD11c^+$ DC, and the extent of fibrosis were investigated by Pearson or Spearman correlation test. All statistical analyses were performed using the SPSS 13.0 for Windows (SPSS Inc). A P value of <0.05 was considered to be significant.

Results

Study Population

All patients were diagnosed with STEMI, and 50% of patients had anterior infarction. Emergent reperfusion therapy was performed in 8% of patients. Mean age was 68±9 years, and 63% of the patients were men. Baseline characteristics of the

Table. Baseline Characteristics of Patients

	Overall (n=24)	Non-Rupture (n=11)	Rupture (n=13)	*P* Value
Age, y	68±9	68±9	69±10	0.66
Male, n (%)	15 (63)	5 (45)	10 (77)	0.21
Smoking, n (%)	13 (56)	5 (45)	8 (62)	0.69
Hypertension, n (%)	20 (83)	10 (90)	10 (77)	0.60
Diabetes, n (%)	8 (33)	6 (55)	2 (15)	0.08
Dyslipidemia, n (%)	5 (21)	2 (18)	3 (23)	1.00
Prior MI, n (%)	5 (21)	4 (36)	1 (8)	0.14
Killip 3 or 4, n (%)	12 (50)	7 (64)	5 (38)	0.41
STEMI, n (%)	24 (100)	11 (100)	13 (100)	
Onset to death, h	167±148	188±164	148±135	0.44
Anterior infarction, %	12 (50)	6 (55)	6 (46)	1.00
Revascularization, %	2 (8)	1 (9)	1 (8)	1.00
White blood cells, $\times 10^3/\mu L$	13.2±5.7	16.5±6.1	10.5±3.6	0.01
Hemoglobin, g/dL	12.1±2.1	12.4±2.8	11.9±1.3	0.60
Peak CPK, $\times 10^3$ IU/L	4.3±4.3	5.7±5.3	2.7±1.5	0.18
Serum creatinine, mg/dL	1.9±2.0	2.6±2.7	1.3±0.6	0.06
Systolic BP, mm Hg	97±34	84±38	108±27	0.07
Diastolic BP, mm Hg	61±23	52±24	67±22	0.19
Heart rate, bpm	78±34	74±45	82±23	0.56

Continuous variables are presented as mean±SD. Categorical variables are presented as number (percentage). BP indicates blood pressure; bpm, beats per minute; CPK, creatine phosphokinase; MI, myocardial infarction; STEMI, ST elevation MI.

study patients including history of prior MI, time from onset to death, rate of reperfusion therapies, and traditional coronary risk factors, but not white blood cell count on admission, were similar in the rupture and non-rupture groups (Table). The time course from onset to death was not significantly different between the two groups (Figure 1).

Extent of Fibrosis and Infiltration of CD68$^+$ Macrophages and CD209$^+$ DC in Infarcted Myocardium

Staining with Masson's trichrome showed decreased %AF of fibrosis in patients with cardiac rupture compared to those without (Figure 2).

Immunohistochemical staining of the infarcted myocardium showed an increase in the number of infiltrating CD68$^+$ macrophages and a decrease in CD209$^+$ DC in patients with cardiac rupture compared with those without (Figure 2).

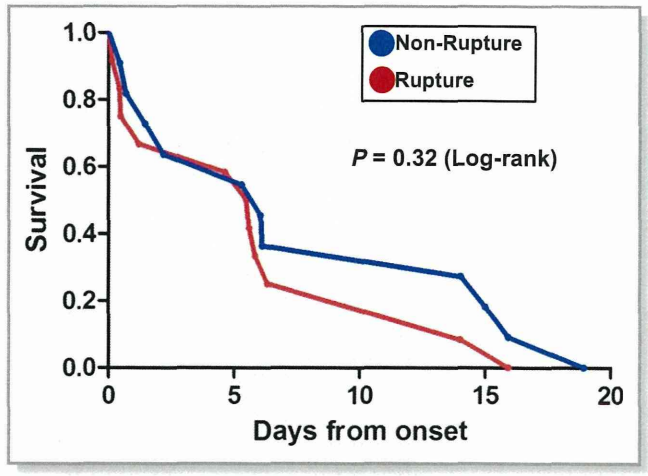

Figure 1. Kaplan-Meier survival analysis in non-rupture and rupture patients after myocardial infarction (MI).

Correlation Among CD68$^+$ macrophages, CD209$^+$ DC and Extent of Reparative Fibrosis

To reveal the possible relationship between inflammatory cell infiltration and the extent of reparative fibrosis, detailed correlation analysis was performed. No significant correlation was found between the number of CD68$^+$ macrophages and% AF of myocardial fibrosis in the infarcted area (R^2=0.01, P=0.39; Figure 3A). However, we found a significant positive correlation between the number of CD209$^+$ DC and %AF of myocardial fibrosis (R^2=0.69, P<0.0001; Figure 3B).

Extent of Fibrosis and Infiltration of CD11c$^+$ DC in Infarcted Myocardium, and Correlation Between CD11c$^+$ DC and Extent of Reparative Fibrosis

To confirm the relationship between DC infiltration and the extent of reparative fibrosis, the same analyses were performed using another DC marker, CD11c.

A decrease in the number of infiltrating CD11c$^+$ DC was observed in patients with cardiac rupture compared to those without (Figure 4A). In addition, we also found a significant positive correlation between the number of CD11c$^+$ DC and % AF of myocardial fibrosis (R^2=0.37, P=0.001; Figure 4B).

Discussion

In the present study, we demonstrated that DC infiltrated human infarcted myocardium after STEMI, and that the degree of infiltration and the extent of reparative fibrosis were significantly lower and the degree of macrophage infiltration was higher in patients with cardiac rupture compared with those without. Interestingly, there was a strong positive correlation between the number of infiltrating DC and the

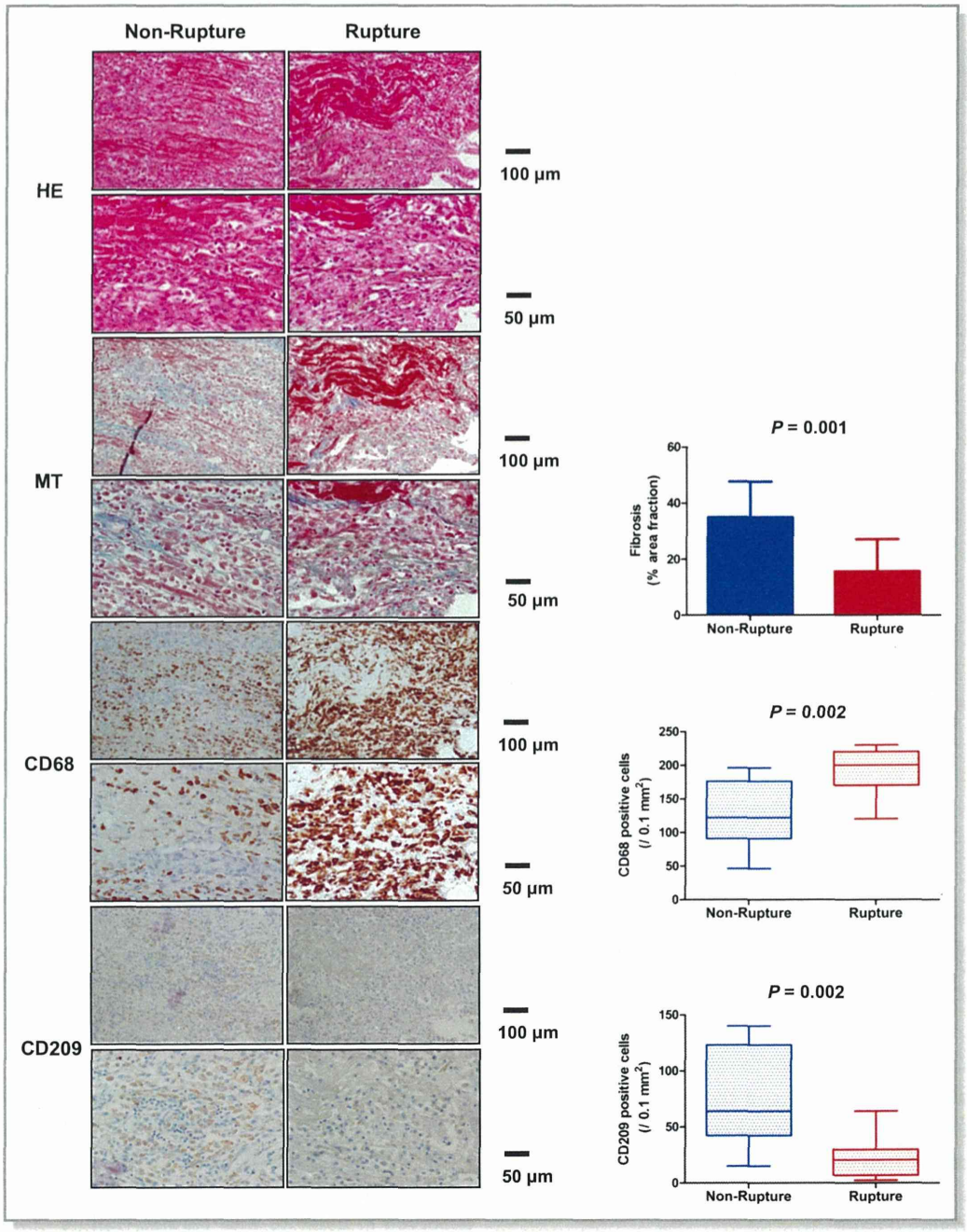

Figure 2. Infiltration of macrophages and DC, and extent of fibrosis in left ventricular infarcted tissue. HE staining, Masson's-Trichrome (MT) staining, immunohistochemical staining for $CD68^+$ macrophages and $CD209^+$ DC in left ventricular infarcted tissue of non-rupture and rupture patients after MI. DC indicates dendritic cells; HE, hematoxylin and eosin; MI, myocardial infarction.

extent of fibrosis in the infarcted myocardium. These findings suggest that DC may play a protective role against cardiac rupture through promotion of reparative fibrosis after MI.

Cardiac rupture is an acute life-threatening complication that occurs in the first several days after MI. Acute myocyte loss and breakdown of extracellular matrix (ECM) promote early ventricular expansion, which is a trigger for subacute cardiac rupture and worsening cardiac function after MI.[9,10] Replacement by collagen is important to provide mechanical stability to the injured tissue, and protects against increased LV dilatation.[11,12] In fact, agents that inhibit collagen synthesis were shown to be associated with an increase in the risk of cardiac rupture in MI patients.[13] These results suggested that appropriate reparative fibrosis is important to prevent cardiac rupture after MI. As well as collagen synthesis, inflammation is also a crucial factor in the

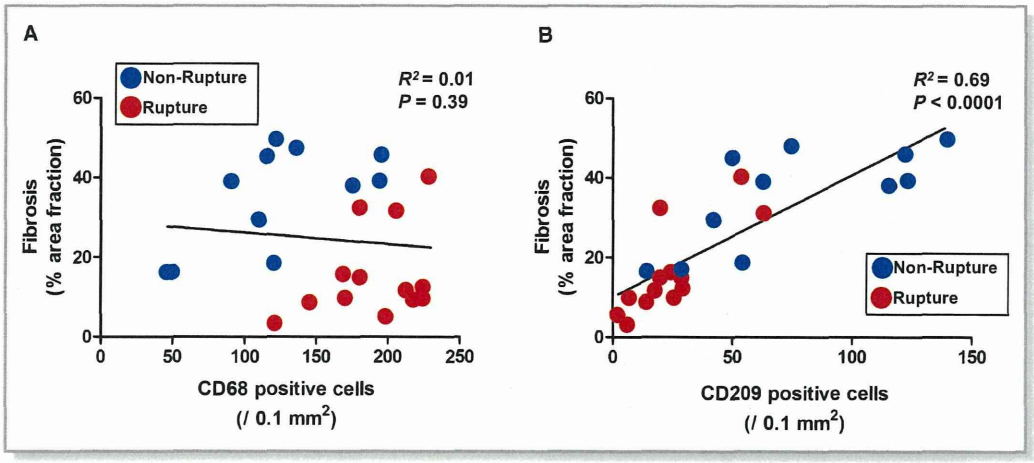

Figure 3. Correlation between extent of fibrosis and infiltration of macrophages and dendritic cells (DC) in left ventricular infarcted tissue. A, Correlation between extent of fibrosis and number of $CD68^+$ macrophages. B, Number of $CD209^+$ DC.

post-MI healing process. An excessive inflammatory response in the infarcted myocardium is related to adverse cardiac events including cardiac rupture;[3,4] however, anti-inflammatory corticosteroid therapy has been reported to increase the incidence of cardiac rupture by delaying collagen accumulation and scar formation, a far from favorable impact on the post-MI healing process.[14,15] These findings indicate that inflammation could be a prerequisite for an adequate post-MI healing process, although excessive inflammation is harmful. Our current study, based on Masson's trichrome staining, showed that the infarcted myocardium in patients with cardiac rupture consisted of disorganized collagen fibers, suggesting the presence of impaired reparative fibrosis. Briefly, impaired reparative fibrosis can be explained by two mechanisms. The first is the degradation of ECM by augmented MMPs secreted from inflammatory cells, predominantly inflammatory monocytes and M1 macrophages, infiltrating the infarcted heart.[7,16,17] Although this process is important for elimination of the necrotic tissue, excessive activation of MMPs could facilitate infarct expansion, resulting in cardiac rupture.[18–21] The second is disordered collagenogenesis by myofibroblasts differentiated from cardiac resident fibroblasts, which are regulated by pro-fibrotic cytokines, such as transforming growth factor beta (TGF-β) secreted mainly from anti-inflammatory monocytes and M2 macrophages during the repair process. M2 macrophages have been reported to promote differentiation of cardiac fibroblasts into myofibroblasts through production of TGF-β.[22] Therefore, adequate regulation of cellular employment is critical for the post-infarction repair process and prevention of cardiac rupture.

DC have come to be appreciated as potent critical controllers that modulate various kinds of inflammatory cells in innate and adoptive immunity.[23–25] Generally, bone-marrow and splenic progenitors and circulating monocytes are reported to differentiate into DC and exert various influences on the immune system at the inflammatory site, such as priming of antigen-specific immune responses, induction of tolerance, and chronic inflammation after tissue injury.[26–28] In the blood, both subtypes of DC are found as circulating DC precursors that lack the expression of costimulatory molecules, so that they are unable to activate other inflammatory cells. In the infarcted myocardium, it was reported that mDC became activated in response to danger signals such as heat shock protein, which is released from necrotic tissue after MI, through the activation of toll-like receptors (TLRs) signaling.[29]

Kretzchmar et al demonstrated a significant decrease in circulating mDC in patients with MI, and also showed significantly higher numbers of markers indicative of mDC and inflammatory cells such as macrophages in the infarcted compared with non-infarcted myocardium. This was accompanied by increased serum levels of an anti-inflammatory cytokine (IL-10) as well as inflammatory cytokines (IL-6, IL-12, and TNFα) in patients with MI.[30] Yilmaz et al also demonstrated that serum high sensitive CRP (hsCRP) and IL-6 levels were decreased, and mDC were partially reconstituted 1 week after the onset in patients with MI. They also showed the number of mDC precursors was negatively correlated with serum hsCRP or IL-6 level, while, in contrast, no significant correlation between pDC precursors and hsCRP or IL-6 was detected.[31] These results suggest that mDC could play important roles in regulating excessive inflammation in the post-MI healing process. Recently, potential mechanisms of suppression of excessive inflammation in a hepatic ischemia-reperfusion mouse model were reported. DC, which were activated by necrotic hepatocytes through TLR9 signaling, might restrict pro-inflammatory monocyte function via production of IL-10.[32] We previously observed mDC infiltrated